Optical Engineering

OpticalEngineering.SPIEDigitalLibrary.org

Dy^{3+}/Tb^{3+}-codoped tunable warm light-emitting fluorogermanate glass phosphor

Rafaela T. Alves
Camyla M. Trindade
Weslley Q. Santos
Artur S. Gouveia-Neto
Luciano A. Bueno
Caio F. Mathias
Marcelo Nalin

SPIE.

Rafaela T. Alves, Camyla M. Trindade, Weslley Q. Santos, Artur S. Gouveia-Neto, Luciano A. Bueno, Caio F. Mathias, Marcelo Nalin, "Dy^{3+}/Tb^{3+}-codoped tunable warm light-emitting fluorogermanate glass phosphor," *Opt. Eng.* **55**(11), 117103 (2016), doi: 10.1117/1.OE.55.11.117103.

Dy^{3+}/Tb^{3+}-codoped tunable warm light-emitting fluorogermanate glass phosphor

Rafaela T. Alves,[a] Camyla M. Trindade,[a] Weslley Q. Santos,[a] Artur S. Gouveia-Neto,[a,*] Luciano A. Bueno,[b] Caio F. Mathias,[c] and Marcelo Nalin[c]
[a]Universidade Federal de Alagoas, Instituto de Física, Maceió, Alabama 57072/970, Brazil
[b]Universidade Federal do ABC, Santo André, CEMCSA, São Paulo 09210580, Brazil
[c]Instituto de Química, UNESP, Araraquara, São Paulo, Brazil

Abstract. Polychromatic tunable visible light emission in the region of the low correlated color temperature range using Dy^{3+}/Tb^{3+} codoped $PbGeO_3:PbF_2:CdF_2$ glass phosphor under UV-blue LED light excitation is presented. The glass phosphor was synthesized and the light emission feature was examined under UV-blue (353, 375, 385, and 405 nm) excitation. Emission around 484, 573, 663, and 754 nm due to dysprosium, and 488, 545, 585, 620, and 690 nm owing to terbium ions, was observed and analyzed as a function of the dysprosium and terbium contents and excitation wavelength. The excitation spectrum was examined and showed resonance peaks around 385 nm for the 573-nm emission of Dy^{3+}, and 375 nm for the 545 nm of Tb^{3+}. Energy-transfer process from $Dy^{3+}(^4F_{9/2})$ to $Tb^{3+}(^5D_4)$ was also observed. Results indicated that the polychromatic visible light emitter herein reported produced light possessing tunable color tone via excitation wavelength and ions' mass ratio. The tint of the tunable overall emission resided in the warm region of the white-light boundary of the CIE-1931 chromaticity diagram.
[DOI: 10.1117/1.OE.55.11.117103]

Keywords: phosphor; rare-earth; white-light emitting diode; solid-state-lightining; polychromatic; warm-light.

Paper 161288 received Aug. 16, 2016; accepted for publication Oct. 12, 2016; published online Nov. 7, 2016.

1 Introduction

A great deal of interest has recently been devoted to the development of a new generation of lighting sources to replace conventional incandescent and fluorescent illuminants. Lighting technology based upon light-emitting diodes (LEDs) incorporates an irreplaceable variety of advantages over daily used incandescent and conventional fluorescent illuminants. They offer much lower energy consumption, apart from being highly reliable, and incorporating environmental-friendly production technology.[1,2] The LED-based lighting systems are regarded nowadays as the next generation solid-state illumination technology[3] since the realization of white LEDs.[4–7] The LED-based sources incorporate valuable properties, which include low power consumption, high electrical energy to light conversion efficiency, long-life, low-cost, and easy maintenance. Moreover, they incorporate environmental advantages because their production does not require emission of greenhouse gases (CO_2) and produces no mercury pollution.[8,9] The approaches to generate white-light using LEDs[1] are basically color addition using LEDs producing the RGB pattern, or visible light multicolor emission from UV/blue excited rare-earth doped phosphor. White LED light via a blueLED and a yellow emitting phosphor is the most utilized approach nowadays, due to the low cost, easy fabrication process, and high brightness emission,[3] despite the fact that this technique suffers from a low color rendering index and the generated white-light changes with excitation power and/or temperature.[10] The absence of red components prevents the generation of light in the red spectral region of the low correlated color temperature (CCT < 3500K). Color tunability includes versatility to the multicolor phosphor for application in the so-called "smart light" technology. Emission color tunability in several rare-earth doped phosphor materials induced via excitation power,[11–13] temperature,[14,15] and adjustment of the active ions' concentration combination has been demonstrated by many.[11,16,17] In the past few years, several reports have been devoted to the search for warm-light emission phosphors using combinations of rare-earth doping including Eu^{3+}/Tb^{3+}, Eu^{3+}/Dy^{3+}, Eu^{3+}/Ce^{3+}, Eu^{3+}/Er^{3+}, Tm^{3+}/Dy^{3+}, $Tm^{3+}/Dy^{3+}/Sm^{3+}$,[17–19,20–27] and in Tb^{3+}/Dy^{3+}-codoped silicate,[28] $CaO\text{-}Al_2O_3\text{-}B_2O_3\text{-}RE_2O_3$,[28] lead-borate,[29] and zinc-phosphate[30] glasses. Bearing that in mind, the search for alternative materials is demanded and fluorogermanate-based glass upsurges as a viable candidate for application in rare-earth doped based upconverters.[31–36] The fluorogermanate host material presents very good optical quality, is stable against atmospheric moisture, and exhibits low optical attenuation in the 0.4 to 5.0-μm spectral region. The material also exhibits high solubility allowing the incorporation of high lanthanide concentrations apart from being nonhygroscopic and possesses high thermal stability against crystallization. In this work, tunable polychromatic light in the low-correlated color temperature range using Dy^{3+}/Tb^{3+}-codoped phosphor is presented. Color tunability was achieved by changing both the concentration and excitation wavelength.

2 Experimental Methods

The Dy^{3+}/Tb^{3+}-codoped glass samples were prepared according to the protocol described in detail elsewhere.[31–35]

*Address all correspondence to: Artur S. Gouveia-Neto, E-mail: artur@fis.ufal.br

0091-3286/2016/$25.00

The synthesis was performed with reagent grade PbF_2 and CdF_2 (P.A. Aldrich) and glassy $PbGeO_3$. Starting reagents were mixed in an agate mortar using n-heptane as the homogenizing medium.[36] After melting in an open Pt-Au crucible at 800°C for 30 min in air, liquids were quenched at room temperature in graphite molds. Some 30 min annealing treatments at temperatures around the glass transition were performed. Rare-earth ions were introduced in the form of oxides (in several different concentrations). Starting $PbGeO_3$ glass was obtained using PbO (P.A. Aldrich) and GeO_2 (P.A. Aldrich) mixed and melted at 800°C for 30 min and quenched to room temperature between two copper plaques. The samples labeled with numbers had concentration combinations as follows: $0.25Dy/x$Tb [$x = 0.25(1)$, 0.50(2), 0.75(3), 1.00 (4)]; $0.50Dy/x$Tb [$x = 0.50(5)$, 0.75(6), 1.00(7)]; and $0.75Dy/x$Tb [$x = 0.50(8)$, 0.75(9), 1.00(10)], in mol%. LED-based excitation sources operating at 353, 375, 385, and 405 nm were employed. The luminescence signal was collected and directed to a fiber-integrated UV-VIS-NIR spectrograph (Ocean Optics HR4000) with an operating resolution of ≤1.0 nm. All spectra presented in this communication were handled employing the proper (Ocean Optics-SpectraSuite) software of the spectrometer. The data were stored and analyzed in a personal computer using commercially available software. The spectra were converted into CIE coordinates using an especially designed software (SPECTRA LUX—Ponto Quântico/RENAMI—Recife—Brazil) to convert and correct the light detector spectral response of the emission luminescence, to CIE-1931 coordinates.

3 Results and Discussion

Figure 1 exhibits the typical excitation spectra for both active ions in the wavelength region of interest of our measurements. The excitation spectra were obtained by exploiting the $^4F_{9/2} \rightarrow {}^6H_{13/2}$ and $^5D_4 \rightarrow {}^7F_6$ of $Dy^{3+}Tb^{3+}$ ions, respectively. The spectra of the main three excitation sources employed in the experiment are also indicated in the figure. Figure 2 shows typical emission spectra of the $80PbGeO_3:10PbF_2:10CdF_2$ phosphors single-doped with Dy^{3+} (1.0 mol%) [Fig. 2(a)] excited at 385 nm and Tb^{3+} (1.0 mol%) excited at 375 nm [Fig. 2(b)].

The emission spectrum [Fig. 2(a)] depicted four distinct visible emission bands around 484 (blue), 573 (yellow), 663 (red), and 754 nm due to dysprosium, which were assigned, respectively, to the electric dipole dysprosium $^4F_{9/2} \rightarrow {}^6H_{15/2}$, $^4F_{9/2} \rightarrow {}^6H_{13/2}$, $^4F_{9/2} \rightarrow {}^6H_{11/2}$, and $^4F_{9/2} \rightarrow {}^6H_{9/2}$ transitions (see energy-level diagram of Fig. 3). Low intensity emission around 835 nm was observed and it was assigned to $^4F_{9/2} \rightarrow {}^6H_{7/2}$. Terbium ions emissions around 383, 488 (blue), 543 (green), 586 (yellow-red), and 620 nm (red) that originated from the $^5D_3 \rightarrow {}^7F_6$, $^5D_4 \rightarrow {}^7F_6$, $^5D_4 \rightarrow {}^7F_5$, $^5D_4 \rightarrow {}^7F_4$, and $^5D_4 \rightarrow {}^7F_3$ transitions (see Fig. 3), respectively, are portrayed in Fig. 2(b). It is important to point out here that there exists an almost resonant overlap region between terbium $^7F_6 \rightarrow {}^5D_4$ absorption spectrum and dysprosium $^4F_{9/2} \rightarrow {}^6H_{15/2}$ emission, which favors the energy-transfer mechanism from Dy^{3+} to Tb^{3+} ions, as indicated in the simplified energy-level diagram of Fig. 3. The dysprosium to terbium energy-transfer process has already been thoroughly investigated[37] and demonstrated elsewhere by many.[28–30] In order to infer the viability of producing warm white-light using other Dy^{3+}/Tb^{3+}-coped fluorogermanate glass phosphor, one has examined the excitation wavelength dependence of the tint of the yellow-reddish light emanating from the dysprosium single-doped samples, as indicated in the graph

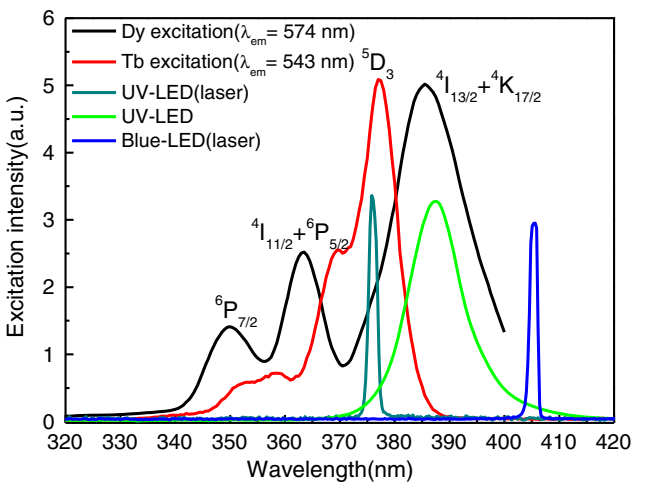

Fig. 1 Excitation spectra of the $80PbGeO_3/10PbF_2/10CdF_2$ glass doped with Dy^{3+} and Tb^{3+} ions. The spectral content of the excitation sources is also indicated in figure.

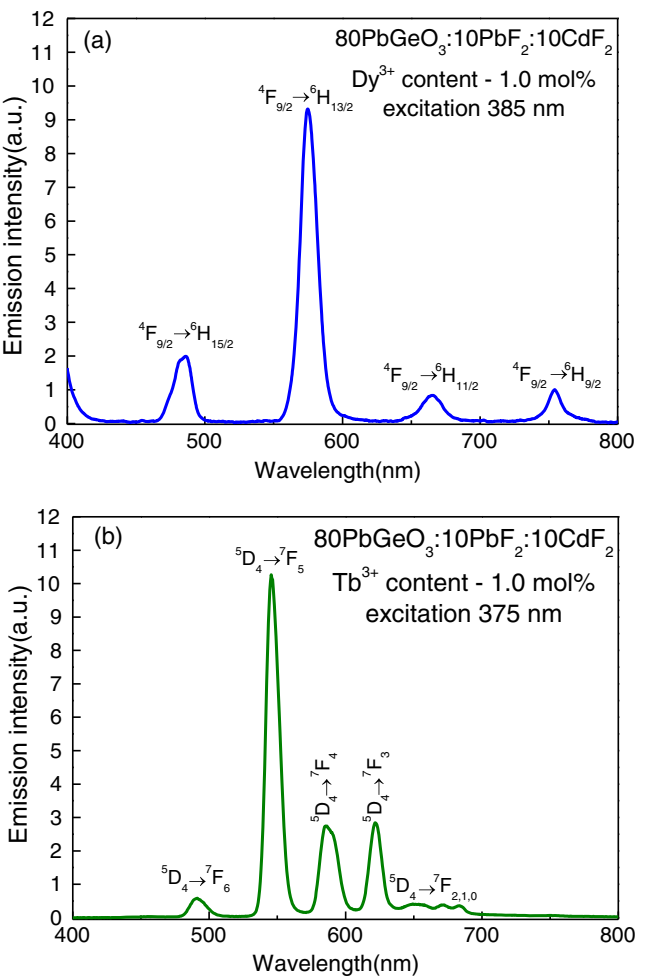

Fig. 2 Emission spectra of the $80PbGeO_3/10PbF_2/10CdF_2$ single-doped with (a) Dy^{3+} and (b) Tb^{3+} ions excited with wavelengths residing in the peak of the excitation curve.

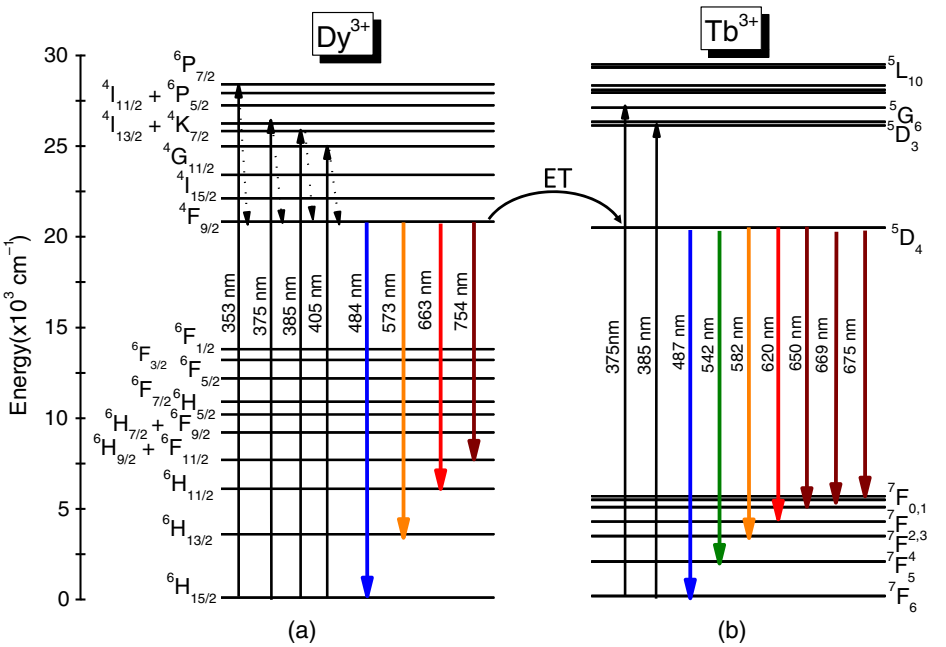

Fig. 3 Simplified energy-level diagram for the (a) Dy^{3+} and (b) Tb^{3+} isolated ions. The upward and downward arrows indicate excitation and emission, respectively. The curved arrow stands for energy-transfer Dy-Tb.

depicted in Fig. 4. As can be seen, the CIE-1931 (X, Y)-coordinates vary substantially from (0.44,0.43) to (0.50,0.46) when the excitation wavelength changes from 353 to 405 nm. The coordinate variation was attributed to the change of the amount of the blue light component generated at different excitation wavelengths, as observed from the spectra of Fig. 4. Tint tunability was also accomplished in double-doped samples via the variation of the Dy^{3+}/Tb^{3+} mass ratios, which caused changes in the relative intensities of color components and also due to the strong energy-transfer process from dysprosium to terbium ions.

Figures 5(a)–5(c) show typical emission spectra of codoped samples under 405-nm diode laser excitation. The excitation wavelength at 405 nm was employed in order to mainly excite dysprosium ions (see Fig. 1) and emphasize the energy transfer Dy^{3+} to Tb^{3+} mechanism. For the excitation wavelength of 405 nm, one has not observed any detectable visible emission from terbium single-doped samples even for the highest excitation power (~16 mW) available in our experiment. As one infers from the data of Fig. 5, the samples with the same Dy^{3+}/Tb^{3+} ions content [Fig. 5(a)] and the spectra show an increasing green component due to terbium ions, while the dysprosium emission components remained almost unchangeable. The inset in Fig. 5(a) containing the CIE-1931 coordinates clearly shows a shift toward the greenish region of the diagram of the overall light emission. The same behavior is observed for the case in which one fixes the terbium content and increases the dysprosium concentration, as portrayed in Fig. 5(b). Here, the energy-transfer process becomes pronounced as the dysprosium emissions decrease in intensity while the terbium green component increases, and as in the first case, a shift toward greenish light has taken place. Finally, Fig. 5(c) illustrates the case for a fixed Dy^{3+} concentration and increasing Tb^{3+} content. Here, the energy transfer from Dy^{3+} to Tb^{3+} is quite noticeable since the green emission intensity owing to terbium ions increased by a factor of ~4.7 while the Tb^{3+} content varies by a factor of 4.0. The Dy^{3+} to Tb^{3+} energy-transfer process can be explained with the help of the simplified energy-level diagram of Fig. 3. The 405-nm excitation promotes the ground-state population of Dy^{3+} ions to the $^4F_{9/2}$ excited level through a one-photon absorption process followed by multiphonon-assisted relaxation. The excited Dy^{3+} decays directly to the $^6H_{15/2}$ ground-state generating 484-nm emission and transfers the remaining part of the energy to the $^5D_4$ level of Tb^{3+} via phonon-assisted electric dipole–dipole interaction, and then the Dy^{3+} relaxes to the ^7F_j lower lying level producing the blue, green, yellowish, and red

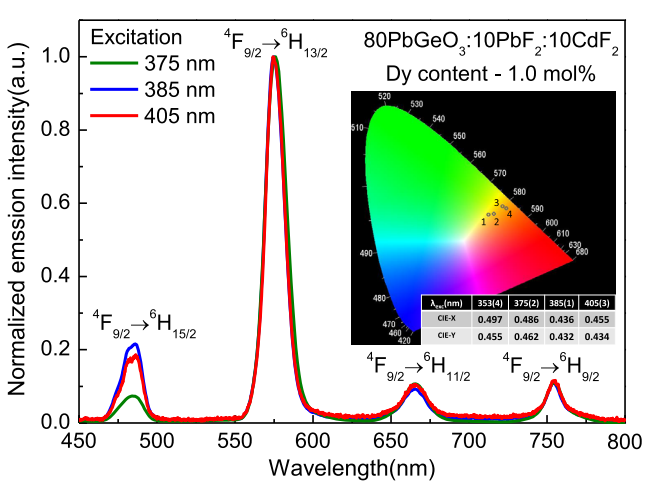

Fig. 4 Emission spectra of dysprosium single-doped samples at different excitation wavelengths. The inset stands for the chromaticity diagram indicating the tunability for different excitation wavelengths.

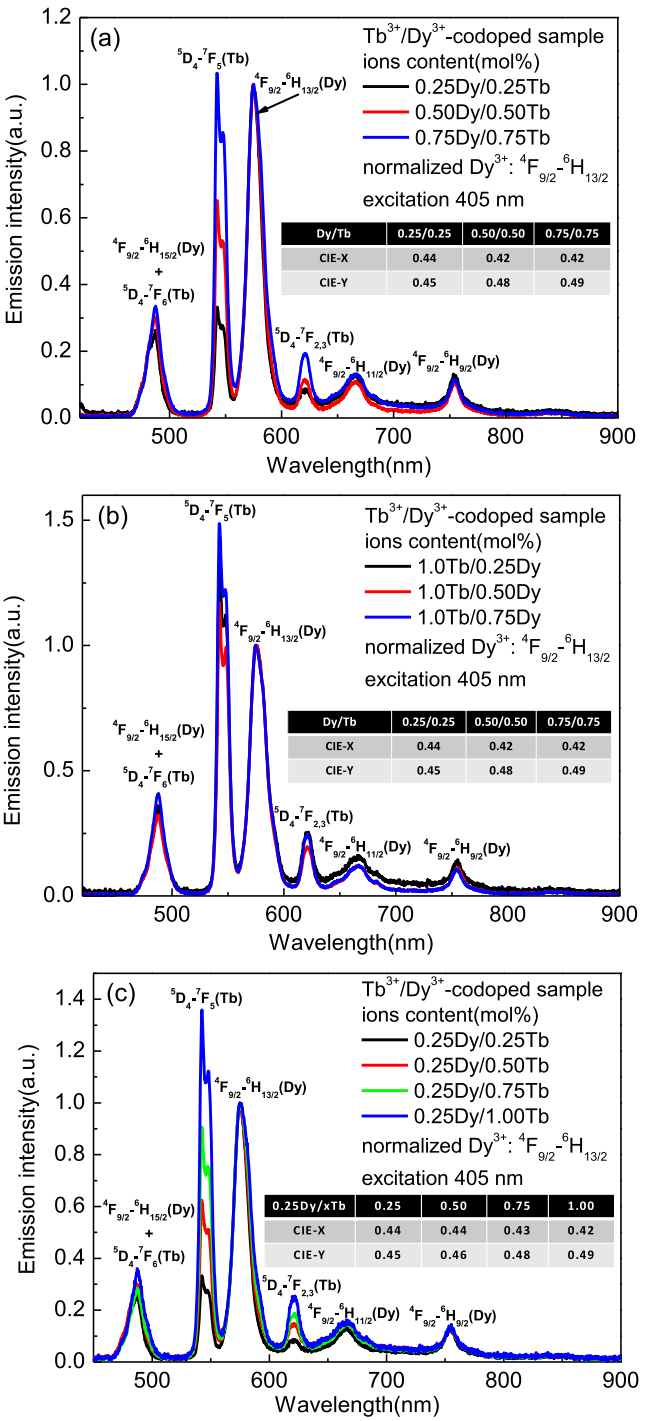

Fig. 5 Emission spectra for the Dy^{3+}/Tb^{3+}-codoped samples excited at 405 nm. (a) samples with equal $Dy^{3+} - Tb^{3+}$ contents, (b) fixed terbium content and varying Dy concentration, and (c) fixed Dy content and changing Tb concentration.

emissions from terbium ions. A back Tb^{3+} to Dy^{3+} energy-transfer process is almost impossible owing to the ~400 cm^{-1} energy mismatch between the $^4F_{9/2}$ and the lower energy $^5D_4$ level of Tb^{3+}.[37] The CIE-1931 coordinates for the samples (1) to (4) using the three excitation wavelengths were then calculated and the results are illustrated in the chromaticity diagram of Fig. 6. As can be seen, the coordinates of the overall emission tint spread out in the

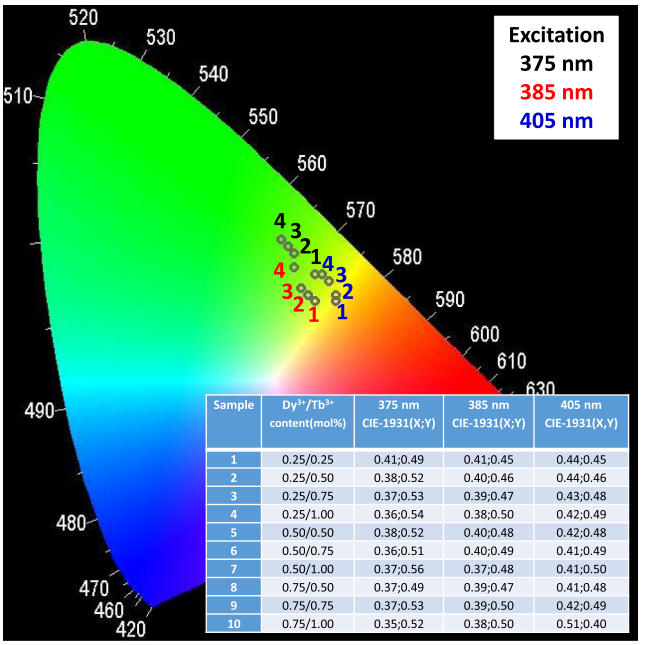

Fig. 6 CIE-1931 chromaticity diagram indicating the coordinates for the (1) to (4) samples at different excitation wavelengths. Numbers 1 to 4 refer to samples (1) to (4), respectively. Inset depicts the table with CIE-1931 coordinates for all samples.

region of the low color-correlated temperature, in particular, the samples (1) and (2) when excited by 385- and 405-nm LED excitation sources. Inset (table) in Fig. 6 presents the CIE-1931 coordinates for all samples excited with the three LED-based sources wavelengths employed in our measurements. The results portrayed in Fig. 6 indicate that indeed the phosphors herein reported produced fluorescence in the low-color correlated temperature and are a viable additional alternative to that reported elsewhere.[38–40] Although the host material utilized in the measurements herein reported contains hazardous elements (Pb, Cd), the lead and cadmium ions are immobilized within the glassy matrix, and further solubility studies in solution with characteristics of the body fluid could confirm this assumption. The use of PbF_2 and of CdF_2 is related to the possibility of the formation of nanocrystals of these fluorides containing rare-earth ions. Thus, the emission of rare-earth ions is more efficient, i.e., the nonradiative transitions are suppressed. The toxicity of heavy metals is extremely reduced as these metals are immobilized inside the glassy matrix. Preliminary studies show that the glassy matrix has low solubility; consequently, metals present in them are cut off from the middle. In the present study, we did not consider comparing the results for the doped glass herein reported with the parent glass. However, a similar study for luminescence in erbium-doped fluorogermanate glass was carried out by us and the results are presented elsewhere.[34,35]

4 Conclusion

Polychromatic tunable visible light emission in the region of the low correlated color temperature range in Dy^{3+}/Tb^{3+}-codoped $PbGeO_3:PbF_2:CdF_2$ glass phosphor was generated. Energy-transfer mechanism between Dy^{3+} and Tb^{3+} was also observed and also influenced the tunability of the overall light emission. Results indicated that the

polychromatic visible light emitter herein reported produced an excitation wavelength tunable color tone in the warm region of the white-light boundary in the CIE-1931 chromaticity diagram.

Acknowledgments

The financial support for this research by CNPq (Conselho Nacional de Desenvolvimento Científico e Tecnológico) under Grant No. 483338/2013-9, FINEP (Financiadora de Estudos e Projetos) CTInfra, Infraspeq 11 and 12, and CAPES (Coordenação de Aperfeiçoamento de Pessoal de Ensino Superior) under Grant No. PVE- AO77/2013 is gratefully acknowledged. R. T. A. and C. M. T. are supported by graduate studentship from Coordenação de Aperfeiçoamento de Pessoal de Ensino Superior. L. A. B. would like to thank the CNPq (grant 486589/2013-7) for financial support.

References

1. E. F. Schubert and J. K. Kim, "Solid-state light sources getting smart," *Science* **308**, 1274–1278 (2005).
2. C. Feldmann et al., "Inorganic luminescent materials: 100 years of research and applications," *Adv. Funct. Mater.* **13**, 511–516 (2003).
3. H. S. Jang and D. Y. Jeon, "Yellow-emitting $SrSiO_5:Ce^{3+}$, Li phosphor for white-light-emitting diodes and yellow-light-emitting diodes," *Appl. Phys. Lett.* **90**, 041906 (2007).
4. S. Nakamura, T. Mukai, and M. Senoh, "Candela-class high-brightness InGaN/AlGaN double hetero-structure bright-light-emitting diodes," *Appl. Phys. Lett.* **64**, 1687 (1994).
5. J. K. Park et al., "White light-emitting diodes of GaN-based $Sr_2SiO_4:Eu$ and the luminescent properties," *Appl. Phys. Lett.* **82**, 683 (2003).
6. J. K. Park et al., "Application of strontium silicate yellow phosphor for white light-emitting diodes," *Appl. Phys. Lett.* **84**, 1647 (2004).
7. J. K. Sheu et al., "White-light emission from near UV InGaN-GaN LED chip precoated with blue/green/red phosphor," *IEEE Photonics Technol. Lett.* **15**, 18–20 (2003).
8. A. Bergh et al., "The promise and challenge of solid-state lighting," *Phys. Today* **54**(12), 42–47 (2001).
9. M. G. Craford, "Visible LEDs: the trend toward high-power emitters and remaining challenges for solid state lighting," *Proc. SPIE* **4776**, 1 (2002).
10. H. Yamamoto, "White LED phosphors: the next step," *Proc. SPIE* **7598**, 759808 (2010).
11. C. H. Liang, Y. C. Chang, and Y. S. Chang, "Synthesis and photoluminescence characteristics of color-tunable BaYZnO:Eu phosphors," *Appl. Phys. Lett.* **93**, 211902 (2008).
12. S.-A. Yan et al., "Synthesis and photoluminescence properties of color-tunable $BaLa_2WO_7:Eu^{3+}$ phosphor," *J. Alloys Compd.* **509**, 5777–5782 (2011).
13. A. S. Gouveia-Neto et al., "White light generation by frequency upconversion in $Tm^{3+}/Ho^{3+}/Yb^{3+}$-codopedfluoroleadgermanate glass," *Appl. Phys. Lett.* **91**, 091114 (2007).
14. D. Chen et al., "Bright upconversion white light emission in transparent glass ceramic embedding in $Tm^{3+}/Er^{3+}/Yb^{3+}:\beta$-$YF_3$nanocrystals," *Appl. Phys. Lett.* **91**, 251903 (2007).
15. H. Gong et al., "Upconversion color tunability and white light generation in in $Tm^{3+}/Ho^{3+}/Yb^{3+}$ doped aluminum germinate glass," *Opt. Mater.* **32**, 554–559 (2010).
16. A. S. Gouveia-Neto et al., "Rare-earth doped solid-state phosphor with temperature induced variable chromaticity," *Mater. Lett.* **63**, 1999–2002 (2009).
17. W. F. Silva et al., "Color tunability with temperature and pump intensity in Yb^{3+}/Tm^{3+} codoped aluminosilicate glass under anti-stokes excitation," *J. Chem. Phys.* **133**, 034507 (2010).
18. D. Chen et al., "Novel rare earth ions-doped oxyfluoridenano-composite with efficient upconversion white-light emission," *J. Solid State Chem.* **181**, 2763–2767 (2008).
19. A. Katelnikovas et al., "Synthesis and optical properties of green to orange tunable garnet phosphors for pcLED," *Opt. Mater.* **33**, 992–995 (2011).
20. R-J Xie and N. Hirosaki, "Eu^{2+}-doped Ca-α-SiAlON: a yellow phosphor for white light-emitting diodes," *Appl. Phys. Lett.* **84**, 5404 (2004).
21. Y. Q. Li et al., "Luminescence properties of red-emitting $MSi5N8:Eu^{2+}$ (M = Ca, Sr, Ba) LED conversion phosphors," *J. Alloys Compd.* **417**, 273–279 (2006).
22. X. Xen et al., "A white light emitting phosphor $Sr_{1.5}Ca_{0.5}SiO_4:Eu^{3+}$, Tb^{3+}, Eu^{2+} for LED-based near-UV chip: preparation, characterization and luminescent mechanism," *J. Lumin.* **131**, 2697–2702 (2011).
23. V. R. Bandi et al., "Luminescence and energy transfer of Eu^{3+} or/and Dy^{3+} co-doped in Sr_3AlO_4F phosphors with NUV excitation for WLEDs," *J. Alloys Compd.* **538**, 85–90 (2012).
24. B. H. Babu and R. K. Kumar, "Warm white light generation in γ-irradiated Dy3, Eu^{3+} codoped sodium aluminoborate glasses," *J. Lumin.* **169**, 16–23 (2016).
25. Q. Du et al., "Novel multiband luminescence of $Y_2Zr_2O_7:Eu^{3+}$, $R^{3+}(R = Ce, Bi)$ orange-red phosphors via a sol-gel combustion approach," *Opt. Mater.* **35**, 257–262 (2012).
26. G. Lakshminarayana, H. Yang, and J. Qiu, "White light emission from Tm^{3+}/Dy^{3+} co-doped oxyfluoride germinate glasses under UV light excitation," *J. Solid State Chem.* **182**, 669–676 (2009).
27. Y. Yu et al., "Color-tunable emission and energy-transfer in $Tm^{3+}/Dy^{3+}/Sm^{3+}$ tri-doped phosphate glass for white light emitting diodes," *Opt. Commun.* **303**, 62–66 (2009).
28. X. Wan et al., "Luminescence and energy-transfer in Dy^{3+}/Tb^{3+} co-doped $CaO\text{-}Al_2O_3\text{-}B_2O_3\text{-}RE_2O_3$ glass," *J. Non Cryst. Solids* **357**, 3424–3429 (2011).
29. J. Pisarska et al., "Energy-transfer from Dy^{3+} to Tb^{3+} in lead borate glass," *Mater. Lett.* **129**, 146–148 (2014).
30. U. Caldino et al., "Down-shifting by energy transfer in Tb^{3+}/Dy^{3+} co-doped zinc phosphate glass," *J. Lumin.* **161**, 142–146 (2015).
31. M. Wachtler et al., "Optical properties of rare-earth ions in lead germanate glasses," *J. Am. Ceram. Soc.* **81**, 2045–2052 (1998).
32. L. A. Bueno et al., "Er^{3+} and Eu^{3+} containing transparent glass ceramics in the system $PbGeO_3\text{-}PbF_2\text{-}CdF_2$," *J. Non Crystall. Sol.* **247**, 87–91 (1999).
33. A. S. Gouveia-Neto et al., "Sensitized thulium blue upconversion emission in $Nd^{3+}/Tm^{3+}/Yb^{3+}$ triply doped lead and cadmium germanate glass excited around 800 nm," *J. Appl. Phys.* **94**, 5678 (2003).
34. A. S. Gouveia-Neto et al., "Red, green, and blue upconversion luminescence in ytterbium-sensitized praseodymium doped lead-cadmium germanate glass," *Opt. Mat.* **26**, 271 (2004).
35. A.O. Silva et al., "Frequency upconversion luminescence in Yb^{3+}-sensitized Er^{3+}- and Pr^{3+}-codoped $PbGeO_3:PbF_2:xF_2$ (x = Mg, Ba) glass," *Opt. Eng.* **55**, 017101 (2016).
36. M. S. Frant and J. W. Ross Jr., "Use of total ionic strength adjustment buffer for electrode determination of fluoride in water supplies," *Anal. Chem.* **40**, 1169 (1968).
37. X-Y Sun et al., "Enhancement of Tb^{3+} emission by non-radiative energy-transfer from Dy^{3+} in silicate glass," *Phys. B* **404**, 111–114 (2009).
38. W. S. Souza et al., "Color tunable green-yellow-orange-red Er^{3+}/Eu^{3+}-codoped $PbGeO_3:PbF_2:CdF_2$ glass phosphor for application in white-LED technology," *J. Lumin.* **144**, 87–90 (2013).
39. J. R. Silva, L. A. Bueno, and A. S. Gouveia-Neto, "Multicolor frequency upconversion luminescence in $Eu^{3+}/Tb^{3+}/Yb^{3+}$-codoped fluorogermanate glass excited at 980 nm," *J. Lumin.* **154**, 531–534 (2014).
40. C. M. da Silva, Jr., L. A. Bueno, and A. S. Gouveia-Neto, "Er^{3+}/Sm^{3+}- and Tb^{3+}/Sm^{3+}-doped glass phosphor for application in warm white light-emitting diode," *J. Non Cryst. Solids* **410**, 151–154 (2015).

Biographies for the authors are not available.